Citation: Cell Death and Disease (2010) 1, e45; doi:10.1038/cddis.2010.24

www.nature.com/cddis

Protein kinase Cθ is required for cardiomyocyte survival and cardiac remodeling

R Paoletti[1,4], A Maffei[2], L Madaro[1], A Notte[2], E Stanganello[1], G Cifelli[2], P Carullo[2], M Molinaro[1], G Lembo[2,3] and M Bouché*[,1]

Protein kinase Cs (PKCs) constitute a family of serine/threonine kinases, which has distinguished and specific roles in regulating cardiac responses, including those associated with heart failure. We found that the PKCθ isoform is expressed at considerable levels in the cardiac muscle in mouse, and that it is rapidly activated after pressure overload. To investigate the role of PKCθ in cardiac remodeling, we used PKC$\theta^{-/-}$ mice. *In vivo* analyses of PKC$\theta^{-/-}$ hearts showed that the lack of PKCθ expression leads to left ventricular dilation and reduced function. Histological analyses showed a reduction in the number of cardiomyocytes, combined with hypertrophy of the remaining cardiomyocytes, cardiac fibrosis, myofibroblast hyper-proliferation and matrix deposition. We also observed p38 and JunK activation, known to promote cell death in response to stress, combined with upregulation of the fetal pattern of gene expression, considered to be a feature of the hemodynamically or metabolically stressed heart. In keeping with these observations, cultured PKC$\theta^{-/-}$ cardiomyocytes were less viable than wild-type cardiomyocytes, and, unlike wild-type cardiomyocytes, underwent programmed cell death upon stimulation with α1-adrenergic agonists and hypoxia. Taken together, these results show that PKCθ maintains the correct structure and function of the heart by preventing cardiomyocyte cell death in response to work demand and to neuro-hormonal signals, to which heart cells are continuously exposed.

Cell Death and Disease (2010) **1,** e45; doi:10.1038/cddis.2010.24; published online 27 May 2010
Subject Category: Experimental medicine

The heart responds to different pathological stimuli, which make it function harder under conditions of hemodynamic overload, by inducing an increase in muscle mass, triggering left ventricular (LV) hypertrophy.[1] This remodeling is considered a compensatory response to the altered workload, allowing the heart to function harder under conditions of sustained stress. However, LV hypertrophy is clinically associated with a significant increase in the risk of heart failure, dilated cardiomyopathy, ischemic heart disease and sudden death, leading to increased cardiovascular mortality. Actually, LV hypertrophy is often followed by LV dilation, which is a reduction in muscle mass, an increase in fibrotic tissue and an enlargement in cavity diameter. This further remodeling results in functional alterations and eventually in the development of heart failure.[1] Many studies have suggested that members of the protein kinase C (PKC) family have a role in cardiac structure. Early studies have shown that TPA, a known PKC activator, activates the fetal gene program and increases cardiomyocyte size.[2,3] However, as the family of serine/threonine protein kinases C comprises at least 12 isoforms, those early studies were somewhat unspecific. Later studies, in fact, showed that many of the PKC isoforms are expressed at appreciable levels in the myocardium and selectively regulate a number of cardiac responses, including those associated with heart failure.[4] PKCs can be subdivided in three subgroups, according to their structure and enzymatic activity: 'conventional' PKCs (PKC α, β1, β2 and γ), the enzymatic activity of which is calcium and phospholipid dependent; 'novel' PKCs (δ, ε, η, θ and μ/PKD), the activity of which is calcium independent but phospholipid dependent; and 'atypical' PKCs (ζ, ι/λ and τ), the activity of which is calcium and phospholipid independent. PKCα activation was found to precede the hypertrophy induced by the overexpression of the L-type voltage-dependent calcium channel in an animal model,[5] and its overexpression in cultured cardiomyocytes induces hypertrophy.[6] By contrast, the absence of PKCα prevents the transition from cardiac hypertrophy to failure.[7] PKCα is not the only PKC isoform involved in the maintenance of cardiac structure. Overexpression of PKCβ1 also induces cardiac hypertrophy and sudden death in animal models, although its ablation does not abolish the hypertrophy induced by either pressure overload or infusion with hypertrophic agonists.[8,9] PKCε is considered the most important isozyme protecting the heart from ischemia and reperfusion injury. Indeed, PKCε overexpression induces cardiac hypertrophy, but with preserved systolic function, suggesting an important role of PKCε for the development of 'compensatory' hypertrophy.[10] PKCθ is

[1]Department of Histology and Medical Embryology, CE-BEMM and Interuniversity Institute of Myology, Sapienza University of Rome, Rome 00161, Italy; [2]Department of Angiocardioneurology, IRCCS Neuromed, Pozzilli (IS), Italy and [3]Department of Experimental Medicine, Sapienza University of Rome, Rome, Italy
*Corresponding author: M Bouché, Department of Histology and Medical Embryology, University of Rome La Sapienza, Via A. Scarpa 14, Rome 00161, Italy.
Tel: +39 06 49766755; Fax +39 06 4462854; E-mail: marina.bouche@uniroma1.it
[4]Current address: CNR-EMMA, Campus Adriano Buzzati-Traverso, Monterotondo, Rome, Italy
Keywords: protein kinase C theta; dilated cardiomyopathy; cardiomyocyte survival; alpha1-adrenergic agonists; protein kinases C
Abbreviations: HDAC, class II histone deacetylase; LV, left ventricular; PKC, protein kinase C
Received 20.1.10; revised 09.4.10; accepted 15.4.10; Edited by RA Knight

known to have a crucial role in T-lymphocyte activation and to mediate various cellular responses in the skeletal muscle.[11–17] However, little is known about PKCθ activity in cardiac function and remodeling. Calcineurin-induced hypertrophic signaling is associated with PKCα and PKCθ activation, both *in vivo* and *in vitro*.[18] In addition, PKCθ has been shown, along with the other members of the 'novel' PKCs subclass, to regulate localization of class II histone deacetylases (HDACs) in different cell systems.[15,19] In the heart, HDACs act as inhibitors of cardiac hypertrophy, and PKC-dependent nuclear export of HDAC5 is a critical event in the signaling cascade in cardiac hypertrophy.[19]

We observed that PKCθ is expressed at considerable levels in the cardiac muscle in mouse, and that it is rapidly activated after pressure overload, suggesting that it may have a role in cardiac response to environmental stimuli. We thus aimed to define the possible role of PKCθ in cardiac structure and function.

Results

PKCθ is expressed in cardiomyocytes, and it is rapidly activated after pressure overload. First, the expression of PKCθ in cardiac muscle was analyzed by double immunofluorescence analysis: as shown in Figure 1A, PKCθ expression is restricted to myosin heavy-chain $(MyHC)^+$ cardiomyocytes. As expected, no PKCθ immunoreactivity was detectable in the PKC$\theta^{-/-}$ hearts (Figure 1A). Moreover, western blot analysis showed that the lack of PKCθ expression did not alter the expression levels of other PKC isoforms, such as PKCα or members of the novel class of PKCs, such as PKCδ, PKCε and PKCη (Figure 1B). To verify whether PKCθ activity may be involved in cardiac remodeling, 10- to 16-week-old WT male mice were subjected to cardiac pressure overload through transverse aortic constriction (TAC). As control, a parallel group of mice was sham operated. After 15 min, the hearts were removed and total,

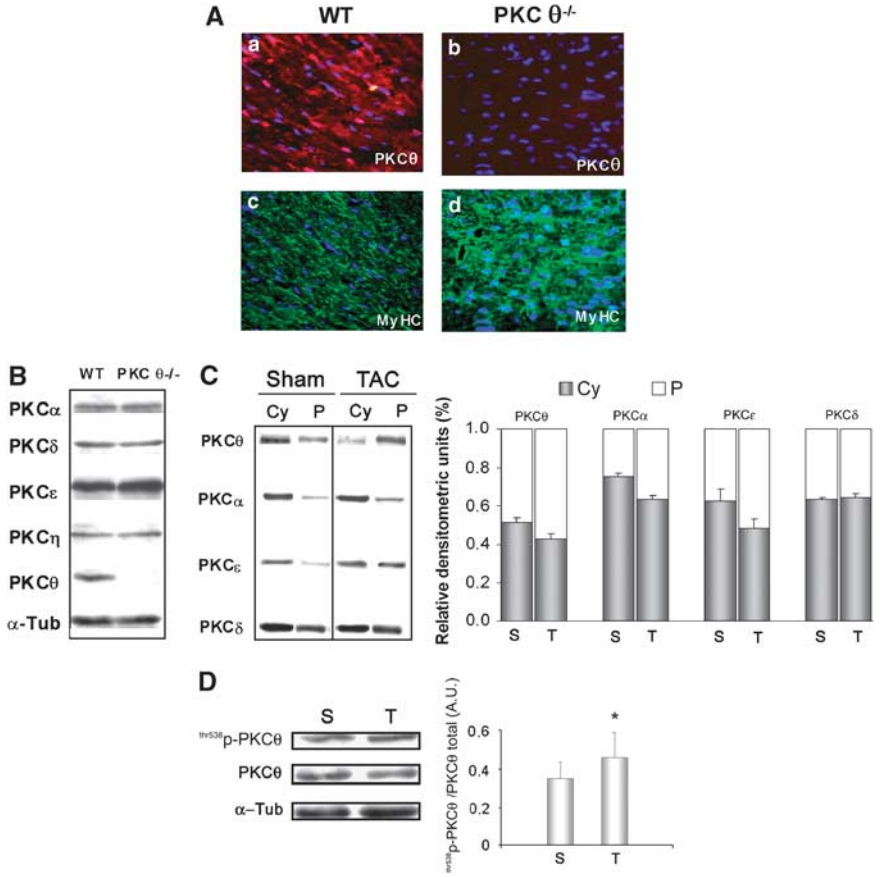

Figure 1 PKCθ is expressed in cardiomyocytes and it is rapidly activated after pressure overload. (**A**) Immunolocalization of PKCθ in cryosections of LV from 2-month-old WT mice (a). Lack of PKCθ expression in PKC$\theta^{-/-}$ LV is shown in b. The α-MyHC MF20 antibody (green) was used to identify cardiomyocytes (c, WT; d, PKC$\theta^{-/-}$). (Bar = 50 μm). (**B**) Western blot analysis of PKC isoforms expression in LV from 2-month-old WT and PKC$\theta^{-/-}$ mice. Representative experiment is shown ($n = 9$ per genotype). The α-tubulin level of expression was used for normalization. (**C**) Left panel: representative western blot of the indicated PKC isoforms content in both cytosolic (Cy) and particulate (P) subcellular protein fractions, after 15 min transverse aortic constriction (TAC). Sham-operated mice (Sham) were used as controls. Right panel: densitometric analysis of the results obtained from western blots of the indicated PKC isoforms content in subcellular protein fractions (empty portion of each column = particulate fraction, P; gray portion = cytosolic fraction, Cy) expressed as relative percentage, with 1.0 given as the total level of expression of each isoform. The results were obtained as the mean value (± S.D.) of western blots prepared from protein subcellular fractions of single animals ($n = 8$ per genotype: 4 sham operated, S, and 4 subjected to TAC, T). (**D**) Western blot analysis of the phosphorylated (active) form of PKCθ (^{Thr538}p-PKCθ) in total protein fractions, after 15 min TAC. The phospho/total PKCθ ratio was evaluated by densitometric analysis and shown in the right. S = sham; T = TAC. *$P < 0.01$

Table 1 Echocardiographic characterization of WT and PKC$\theta^{-/-}$mice

Parameter	WT	PKC$\theta^{-/-}$
RRs (mm Hg)	107 ± 4	117 ± 3
LVID (mm)	3.185 ± 0.16	3.74 ± 0.40
LVPW (mm)	0.72 ± 0.02	0.60 ± 0.08
IVS (mm)	0.74 ± 0.02	0.61 ± 0.07
FS (%)	53.9 ± 3.8	38.07 ± 7.8*
LV%EF	82.5 ± 2	68 ± 2.2*

RRs, systolic blood pressure; LVID, left ventricular end-diastolic diameter; LVPW, left ventricular posterior wall thickness in end diastole; IVS, interventricular septum thickness in end diastole; %FS, percentage fractional shortening; LV%EF, left ventricular percentage ejection fraction. *$P<$ 0.01 *versus* WT.

Table 2 Hemodynamic parameters in WT and PKC$\theta^{-/-}$ mice

Parameter	WT	PKC$\theta^{-/-}$
HR, b.p.m.	269.5 ± 22.0	291.8 ± 18.1
ESV, μl	24.2 ± 2.6	44.1 ± 5.9*
EDV, μl	64.6. ± 3.9	75.8 ± 8.2
Systolic function		
Max pressure, mm Hg	88.8 ± 4.4	89.9 ± 5.5
ESP, mm Hg	82.6 ± 4.7	82.1 ± 5.5
dP/dtmax, mm Hg per s	5249 ± 380	5238 ± 526
EF, %	67.5 ± 1.9	49.2 ± 1.7*
SV, μl	46.4 ± 2.0	37.8 ± 2.8*
Ees, mm Hg/μl	1.7 ± 0.3	0.9 ± 0.2*
Diastolic function		
EDP, mm Hg	4.6 ± 0.8	6.0 ± 1.5
dP/dtmin, mm Hg per s	−3994 ± 477	−4851 ± 591
τ (Glantz), msec	21.0 ± 2.1	16.0 ± 1.1
EDPVR, mm Hg/μl	0.2 ± 0.1	0.3 ± 0.1

HR, heart rate; ESV, end-systolic volume; EDV, end-diastolic volume; ESP, end-systolic pressure; EF, ejection fraction; SV, stroke volume; Ees, elastance, end-systolic; EDP, end-diastolic pressure; EDPVR, end-diastolic pressure–volume relationship. *$P<0.05$ *versus* WT.

soluble and particulate (membrane) protein fractions were prepared for western blot analysis. As shown in Figure 1C, PKCθ rapidly translocated to the membrane fraction after TAC. Among the other isoforms analyzed, both PKCα and PKCε, the activation of which is known to be linked to cardiac hypertrophic response, also translocated to the membrane fraction, whereas no PKCδ membrane translocation was observed, after 15 min of TAC. PKCθ activation was also confirmed by western blot analysis using an anti- ^{Thr538}p-PKCθ-specific antibody: after TAC, a higher fraction of the total PKCθ is phosphorylated (activated) as compared with sham-operated hearts (Figure 1D).

The lack of PKCθ expression results in LV dysfunction. To assess the effect of the lack of PKCθ expression on cardiac structure and function, echocardiographic analyses were performed in 10- to 16-week-old male mice compared with age- and sex-matched WT mice (10 mice per genotype). LV diameters, wall thickness and contractile function were evaluated at basal conditions. LV from PKC$\theta^{-/-}$ mice displayed reduced wall thickness and enlarged diameter, when compared with WT mice (Table 1). These findings are consistent with a pathological phenotype of dilated cardiomyopathy. As expected, a significant reduction in contractile performance was observed. Indeed, ablation of PKCθ induced a 25–29% reduction in fractional shortening, associated with a parallel reduction in ejection fraction (Table 1). This defect in contractility was confirmed by the more accurate hemodynamic analysis of the pressure–volume curves (Table 2), which showed that end-systolic volume was increased, whereas stroke volume and end-systolic elastance were decreased in PKC$\theta^{-/-}$ mice, when compared with WT mice.

The lack of PKCθ expression induces cardiac fibrosis. To identify the LV characteristics that led to the observed cardiomyopathic phenotype, we performed histological analyses on the hearts of PKC$\theta^{-/-}$ and WT mice. Gomori's trichrome staining of 2-month-old PKC$\theta^{-/-}$ LV cryosections revealed a significant increase in interstitial fibrosis when compared with age-matched WT LVs (Figure 2A). RT-PCR showed that the observed fibrosis was associated with an increase in the expression of *collagens 1α1* and *3α1* (the main constituents of the cardiac extracellular matrix), as well as of α-*SMA*, a primary marker of fibroblast-to-myofibroblast conversion and *TGFβ*, a fibrogenic growth factor (Figure 2B). Quantification of the fibrosis areas at different time points during postnatal life showed that in newborn mice, there was no significant increase in fibrosis in the LVs of either genotype; by contrast, a highly significant increase in the accumulation of interstitial fibrosis in PKC$\theta^{-/-}$ mice was observed with age, when compared with age-matched WT mice (Figure 2C).

To determine whether this increased fibrosis was due to the altered proliferation/activity of cardiac fibroblasts (CFs), cell proliferation was evaluated *in vivo* by 5-bromo-2′-deoxyuridine (BrdU) incorporation. Figure 3A shows that a significant increase in the percentage of BrdU^{+ve} cells was evident in 2-month-old PKC$\theta^{-/-}$ hearts, compared with WT hearts, and that BrdU^{+ve} cells were localized in interstitial, myosin^{-ve} areas, and can thus be regarded as CFs. The increased cell proliferation in PKC$\theta^{-/-}$ hearts was also confirmed by the increase in *PCNA* (a marker of the S phase) and *Cyclin D1* (a marker of the G1/S phase transition) expression, as revealed by RT-PCR analysis (Figure 3A). To confirm that PKCθ ablation leads to proliferation of CFs, these cells were also isolated from LVs of 1- to 3-day-old mice and their proliferation capability was analyzed *in vitro*. As shown in Figure 3B, a 60% increase in BrdU^{+ve} cells was observed in cultured PKC$\theta^{-/-}$ CFs, when compared with WT CFs. This increase was associated with a significant upregulation of *Coll 1α1* expression.

The lack of PKCθ expression induces hypertrophy of cardiomyocytes but reduces their number. Hematoxylin/eosin staining of LV from 2-month-old mice also showed that the cardiac fibrosis we observed was associated with an increase in cardiomyocyte size (Figure 4A). The cross-sectional area (CSA) of LV cardiomyocytes was evaluated by α-caveolin-3 (cardiomyocyte-specific) immunofluorescence, at different time points during postnatal life. As shown in Figure 4B, cardiomyocyte CSA was increased in PKC$\theta^{-/-}$

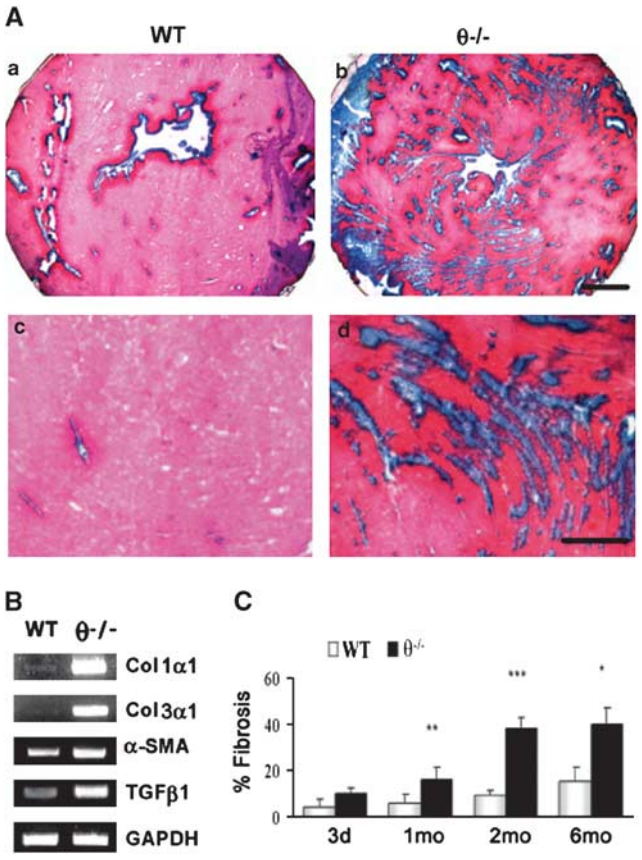

Figure 2 PKCθ ablation results in increased fibrosis. (**A**) Gomori's trichrome-stained representative cryosections of LV from 2-month-old WT (a and c) and PKC$\theta^{-/-}$ mice (b and d); a–b: bar = 2 mm; c–d: bar = 200 μm. (**B**) RT-PCR analysis of the indicated fibrotic markers in LVs from 2-month-old WT and PKC$\theta^{-/-}$ mice (3 mice per genotype). *Col1α1*: *α1 collagen 1*; *Col3α1*: *α1 collagen 3*; *αSMA*: *α-smooth muscle actin*; *TGFβ1*: *transforming growth factor β1*; *GAPDH* expression was used to normalize the reaction. (**C**) Quantification of interstitial fibrosis was examined at the indicated postnatal ages of WT (empty bars) and PKC$\theta^{-/-}$ (filled bars) LVs, expressed as a percentage of the total area of the entire section. At least three sections per mouse were analyzed ($n = 3$ per genotype/age). *$P < 0.01$; **$P < 0.001$; ***$P < 0.0001$

mice at all ages examined. Moreover, this increase in cardiomyocyte size was associated with a significant reduction in the number of cells at all ages examined. In fact, as shown in Figure 4B, θ-ablation resulted in a reduction in the number of cardiomyocytes, ranging from 10%, at 1 month of age, up to 25% in subsequent growth phases, when compared with age- and sex-matched WT mice.

Thus, we analyzed signaling proteins involved in cardiomyocyte death in response to hypertrophic and stress stimuli, namely p38 and JNK mitogen-activated protein (MAP) kinases.[20] We observed that p38 and JNK phosphorylations were both markedly higher in 2-month-old PKC$\theta^{-/-}$ LVs than in WT LVs. By contrast, phosphorylation levels of ERK1/2, which is implicated in cell proliferation/survival, were not altered (Figure 4C). Moreover, we analyzed the activation of a fetal gene expression program, which is usually associated with pathological LV remodeling. RT-PCR analysis showed that the expression of genes encoding atrial natriuretic factor (*ANF*), *α-skeletal actin* (*α-SKA*) and the fetal *β-myosin heavy chain* (*β-MyHC*), although barely detectable in LVs from 2-month-old WT mice, was high in LVs from age- and sex-matched PKC$\theta^{-/-}$ mice (Figure 4D). Moreover, in PKC$\theta^{-/-}$ LVs, the increased *α-SKA* mRNA level was associated with decreased *α-cardiac actin* (*α-CAA*) expression, when compared with WT LVs, where *α-CAA* isoform expression accounts for most of the actin expressed (Figure 4D). Interestingly, although the low level of *α-SKA* expression remained constant in LVs from WT mice, a progressive age-related increase was observed in the *α-SKA* transcript level in PKC$\theta^{-/-}$ hearts (data not shown).

PKCθ is required for cardiomyocyte survival. Next, we investigated whether the phenotype we observed was due to an impaired sensitivity to extracellular signals, to which heart cells are continuously exposed and which leads to cardiomyocyte death. Thus, we analyzed the adaptive response of cultured cardiomyocytes to such signals. Neonatal CMCs were isolated from 1- to 3-day-old PKC$\theta^{-/-}$ and WT mice. Morphological analysis showed that PKC$\theta^{-/-}$ CMCs were significantly larger (by ~50%) than WT CMCs (Figure 5A and B), reflecting the size increase observed *in vivo*. Moreover, actin filament organization resembled a hypertrophic phenotype, forming 'stress fiber-like structures', as shown by F-actin staining with phalloidin (data not shown). To examine the role of PKCθ in the adaptive response of CMCs to work demand, CMCs were stimulated with phenylephrine (PE), the α1-adrenergic agonist. As expected, after 48 h of treatment, WT CMCs increased in size, reaching a size similar to that observed in untreated PKC$\theta^{-/-}$ CMCs. Accordingly, ANF expression was not detectable in untreated WT CMCs, whereas PE treatment induced evident perinuclear ANF protein accumulation. By contrast, upon agonist exposure, size was significantly reduced in PKC$\theta^{-/-}$ CMCs (Figure 5A and B). Moreover, the perinuclear ANF protein accumulation, already evident in untreated PKC$\theta^{-/-}$ CMCs, was significantly reduced upon exposure to the agonist (Figure 5A). Similar results were obtained when CMCs were exposed to endothelin-1 or angiotensin II (data not shown).

To investigate the 'pathological' response to hypertrophic stimuli, the expression and activation of factors involved in the hypertrophic transduction pathways were analyzed in both WT and PKC$\theta^{-/-}$ CMCs, either treated with or without PE. As expected, when WT CMCs were treated with PE for 30 min, a significant 30% increase in Akt phosphorylation was observed by western blot analysis as a result of the hypertrophic response. By contrast, no increase in Akt phosphorylation was observed in PKC$\theta^{-/-}$ CMCs upon PE treatment. (Figure 5B).

When WT CMCs were treated with PE for longer periods of time (48 h), an increase in both the *ANF* and *MyHC* expression levels was observed, as expected. By contrast, the higher basal expression level of both *ANF* and *MyHC* in PKC$\theta^{-/-}$ CMCs, if compared with that of WT CMCs, was reduced by the treatment (Figure 5B). Moreover, western blot analysis showed that cardiac troponin I (cd-TnI) intracellular content was significantly lower (~30%) in PKC$\theta^{-/-}$CMCs than in WT CMCs, and was further reduced upon PE treatment (Figure 5B). No significant differences in cd-TnI expression

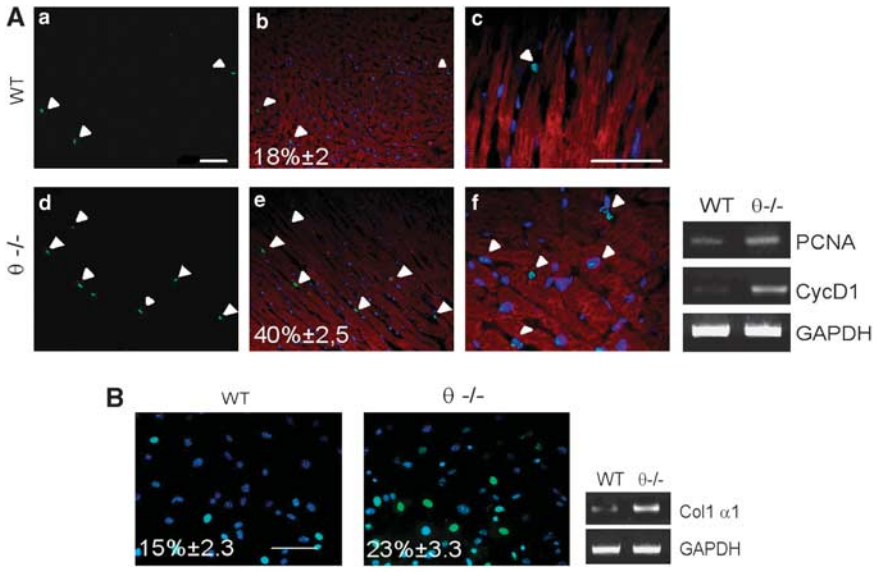

Figure 3 PKCθ ablation results in increased fibroblast proliferation. (**A**) BrdU incorporation (green) in 2-month-old WT (a–c) and PKC$\theta^{-/-}$ (d–f) LVs. Sections were counterstained with Hoechst and α-MyHC antibody (red) (b–c and e–f). Representative micrograph of transverse sections at higher magnification is shown in c and f (bar = 50 μm). The percentage of BrdU^{+ve} nuclei per section over the total number of nuclei is also shown ($P<0.01$ *versus* WT; $n=3$ per genotype). RT-PCR analysis of *PCNA* and *Cyclin D1* expression in 2-month-old WT and PKC$\theta^{-/-}$ LVs is shown in the right. *GAPDH* expression was used to normalize the reaction. (**B**) Immunofluorescence analysis of BrdU incorporation in cultured CFs isolated from LV of 1- to 3-day-old WT and PKC$\theta^{-/-}$ mice (bar = 50 μm). The percentage of BrdU^{+ve} nuclei per microscopic field over the total number of nuclei is also shown ($P<0.01$ *versus* WT). RT-PCR analysis of *Coll 1α1* expression in WT and PKC$\theta^{-/-}$ cultured CFs is shown in the right. *GAPDH* expression was used to normalize the reaction

were observed in WT CMCs, regardless of whether they were exposed to PE. Degradation and/or release of regulatory myofibrillar proteins, such as cd-TnI or cd-TnT, are known to occur upon cardiomyocyte damage.[21]

Trypan blue and TUNEL analyses were then used to investigate whether treatments induced cell death in PKC$\theta^{-/-}$ CMCs (Figure 5C). At basal conditions in serum-free medium, the percentage of PKC$\theta^{-/-}$ CMCs permeable to trypan blue was already 2.5 times higher than in WT cells. PE exposure (48 h) resulted in a further increase in the percentage of trypan blue-positive CMCs, when compared with untreated PKC$\theta^{-/-}$ CMCs. No differences were observed in WT cells upon treatment. Similar results were obtained when CMCs were exposed to endothelin-1 or angiotensin II, as well as to environmental stress stimuli, such as hypoxic conditions (data not shown). To verify whether the observed cell death was due to protease activity, CMCs were treated with leupeptin (Leu), a protease inhibitor preferentially active on calpains, before being exposed to PE. A 30-min Leu pretreatment, followed by 48 h of exposure to PE, significantly reduced trypan blue-positive PKC$\theta^{-/-}$ CMCs to a level comparable with WT CMCs (Figure 5C).

TUNEL analysis was performed to assess whether the cell death we observed was due to apoptosis. At basal conditions in serum-free medium, the percentage of TUNEL-positive nuclei was already higher in PKC$\theta^{-/-}$ than in WT cells (Figure 5D). PE exposure (48 h) induced, in PKC$\theta^{-/-}$ CMCs, a further increase (about three times) in the percentage of apoptotic nuclei, if compared with unstimulated cells. By contrast, no increase was detectable in PE-treated WT CMCs (Figure 5D). Similar results were obtained using endothelin-1 and angiotensin II treatments (data not shown).

To characterize which apoptotic pathway is active in the absence of PKCθ, PKC$\theta^{-/-}$ and WT CMCs were treated with or without PE for 4 h; cleavage of caspase-9 and caspase-8 was analyzed by western blot. As shown in Figure 5E, the caspase-9 proteolitic fragment (p35/36, the active form) was evident in untreated PKC$\theta^{-/-}$ CMCs, and it was further accumulated after 4 h PE treatment. Very little, if no, caspase-9 cleavage was observed in WT CMCs, and PE exposure induced a slight increase in p35/36 accumulation. By contrast, no cleaved/active fragments of caspase-8 were detectable in both WT and PKC$\theta^{-/-}$ CMCs, although a slight increase in full-length caspase-8 accumulation was evident after 4 h PE, in both WT and PKC$\theta^{-/-}$ CMCs to a similar extent.

Discussion

In this paper, we show that the expression/activity of the θ-isoform of PKCs ensures the correct structure and function of cardiac muscle, at least in part, by protecting cardiomyocytes from cell death.

As first, PKCθ is expressed at a considerable level in mouse cardiomyocytes; moreover, it is strongly activated, together with PKCα and PKCε, within 15 min of aortic banding, suggesting that it may have a pivotal role in the cardiac response to pressure overload. Both PKCα and PKCε have been implicated in cardiac hypertrophy, based on *in vivo* and *in vitro* studies, although they probably have different roles.[4] In particular, PKCα is supposed to be involved in the transition from hypertrophy to heart failure, whereas PKCε is believed to be involved in compensatory hypertrophy.[7,22] The fact that both isoforms are rapidly (within 15 min) activated upon pressure overload, which has never been investigated before,

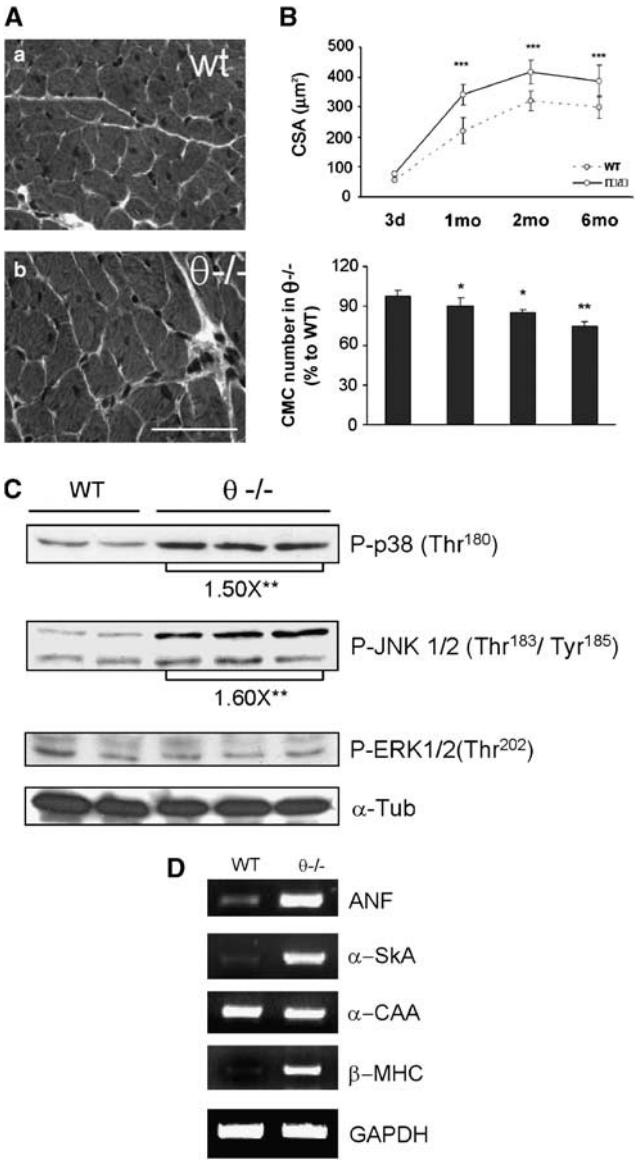

Figure 4 PKCθ ablation induces CMC hypertrophy and loss, MAPK activation and reexpression of cardiac fetal genes. (**A**) Representative images of H&E staining of cryosections obtained from 2-month-old WT (a) and PKC$\theta^{-/-}$ (b) mice LVs (bar = 50 μm). (**B**) Top panel: mean CMC CSA in WT and PKC$\theta^{-/-}$ LVs at different time points during postnatal growth (d = days, mo = months); 40 microfields per mouse (~2000 myocytes each group) were analyzed, $n = 3$ each group. Bottom panel: the number of CMCs in PKC$\theta^{-/-}$ LVs at different time points during postnatal growth, expressed as the percentage of the number of CMCs in age-matched WT LVs, with the number of WT CMCs considered as 100 (*$P<0.01$, **$P<0.001$, ***$P<0.0001$ *versus* WT). The number of CMCs in the heart was determined by counting caveolin-3 and myosin $^{+ve}$ cells in 50 microscopic fields per cryosection ($n = 3$ each group). (**C**) Western blot analysis of the indicated phospho-MAPKs in LV protein extracts from 2-month-old WT and PKC$\theta^{-/-}$ mice. The representative experiment is shown. Relative fold inductions are shown, as determined by densitometric analyses of western blots from three independent experiments ($n = 9$ per genotype), using α-tubulin expression for normalization (**$P<0.001$ *versus* WT). (**D**) RT-PCR analysis of the expression of *ANF* (*atrium natriuretic factor*), α-*SKA* (α-*skeletal actin*), α-*CAA* (α-*cardiac actin*), β-*MyHC* (β-*myosin heavy chain*) in 2-month-old WT and PKC$\theta^{-/-}$ LVs. GAPDH expression was used to normalize the reaction

indicates that the actual outcome of the stimulus (maladaptive or compensatory hypertrophy) depends on a delicate balance between the different pathways. Interestingly, PKCδ, the activity of which has been proposed to be somehow redundant to PKCε activity with respect to cardiac hypertrophy,[22] does not change. This observation suggests that, unlike PKCε, PKCδ is not involved in the early response to pressure overload and does not behave exactly as PKCε. Moreover, PKCδ is structurally related to PKCθ, which behaves similarly to PKCε to pressure overload, instead. Whether PKCθ and PKCε, which belong to the same PKC subfamily as PKCδ, may have similar or specific roles in the response of heart to pressure overload will need further investigation.

However, the data reported in this paper show that the lack of PKCθ expression *in vivo* results in basal cardiac dysfunction, differently from what occurs in the absence of PKCε,[23] highlighting a possible distinguished and specific role for PKCθ in cardiac structure and function under physiological conditions. Indeed, PKC$\theta^{-/-}$ mice exhibit abnormalities in several contractility indexes. In particular, the lack of PKCθ expression affects the ejection phase of the LV systole, although it does not have any effect on the diastole or on the isovolumic phase of systole. On this issue, indexes of the ejection phase have been identified as the most reliable parameter for detecting depressed myocardial function.[24] This loss of cardiac function is associated with a structural defect, consisting of reduced wall thickness and greater LV diameter. The combination of dilation and thinner muscle wall reduces the efficiency of heart performance, which results in lower contractile power per cardiac area. It is noteworthy that in most of the animal models, lacking or overexpressing specific PKC isoforms, altered cardiac function is only evident in response to pathological stimuli.[4,23,25] Even ablation of PKCε, which is considered the most important isozyme protecting the heart from ischemia and reperfusion injury, did not exert any basal cardiac phenotype, although the combination of loss- and gain-of-function approaches, aimed to modulate its translocation, suggested a role for PKCε signaling in normal postnatal maturational myocardial development, probably regulating cardiomyocytes proliferation.[22,23] This fact suggests that most PKC isoforms are modifiers of heart response to specific stimuli, or that the eventual redundancy between them can preserve basal physiology in mutant models. By contrast, the absence of PKCθ affects the normal physiology of the heart. Thus, PKCθ, differently from any other isoform, may be considered a key protein for cardiac structure and function under physiological conditions. Moreover, the cardiomyopathy observed in PKC$\theta^{-/-}$ mice is associated with a profound alteration in the cellular and extracellular structure of the heart. Indeed, increased interstitial fibrosis was observed in the absence of PKCθ. This increase occurs during postnatal heart growth, as demonstrated by the fact that no differences were observed in the hearts of newborn mice and that fibrotic areas increased with age. This is the result of increased myofibroblast proliferation and matrix deposition, as shown by both *in vivo* and *in vitro* analyses, possibly as a consequence of the progressive loss of cardiomyocytes observed in the hearts lacking PKCθ. As a result, the surviving cardiomyocytes

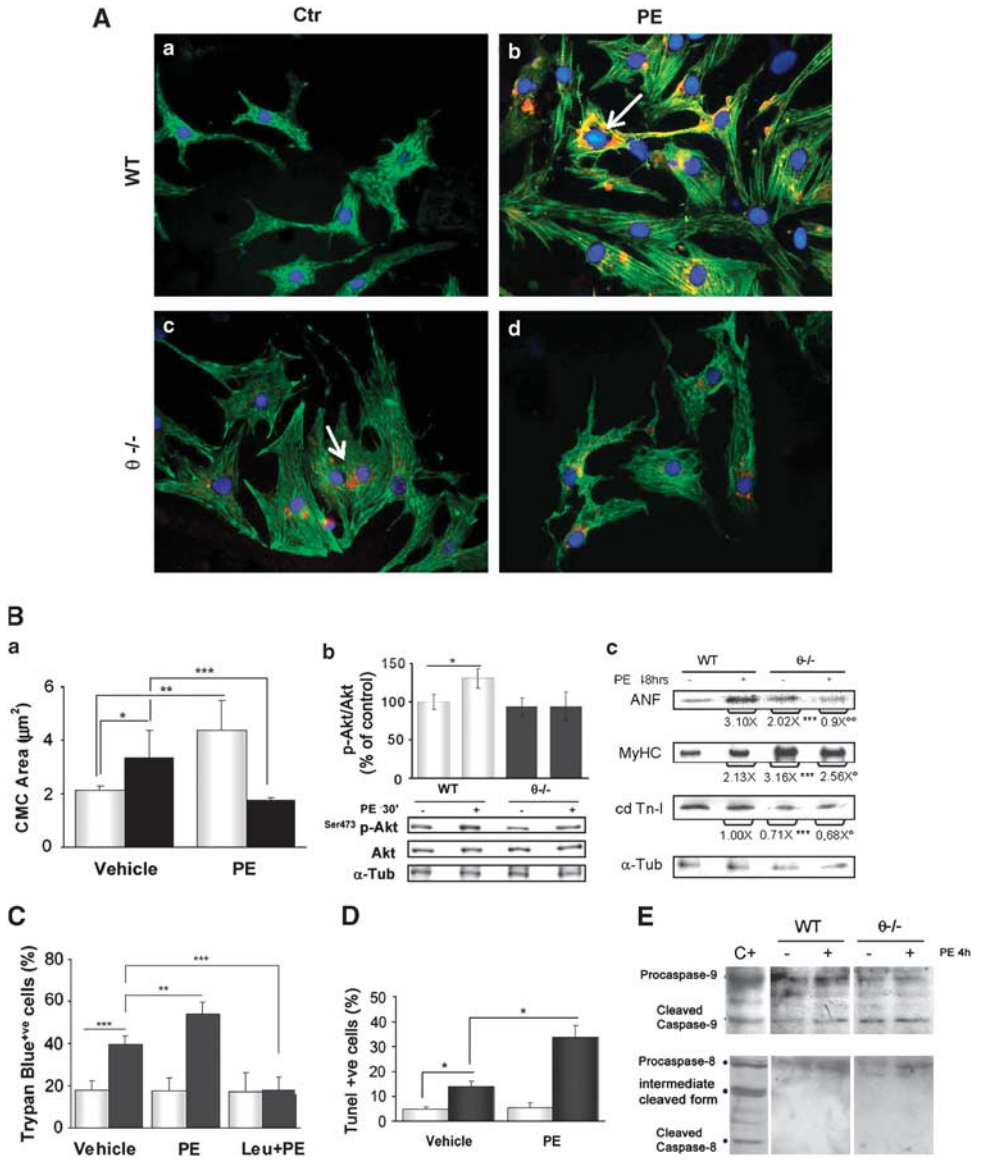

Figure 5 PKCθ ablation sensitizes CMCs to stress-induced cell death. (**A**) Immunofluorescence analysis of serum-starved WT (a–b) and PKC$\theta^{-/-}$ CMCs (c–d), either treated (b and d) or not treated (a and c) with PE for 48 h, using α-MyHC (green) and α-ANF (red) antibodies (arrows show perinuclear ANF protein expression). (**B**) (a) Area determination in cultured WT and PKC$\theta^{-/-}$ CMCs, either treated with or without PE for 48 h. CMC area was measured in MF20^{+ve} cells using the Scion Image Program ($n = 1000$ cells per each condition; $^{*}P < 0.01$, $^{**}P < 0.001$, $^{***}P < 0.0001$); (b) western blot analysis of WT and PKC$\theta^{-/-}$ CMCs, treated with or without PE for 30 min., as indicated The blot was incubated with the α-Akt or the α-phospho-Akt antibodies. The level of activation was determined by densitometric analysis, as the phospho/total Akt ratio ($^{*}P < 0.01$). Tubulin level of expression was used to ensure equal loading; (c) western blot analysis of WT and PKC$\theta^{-/-}$ CMCs, treated with or without PE for 48 h, as indicated. The blot was incubated with the α-ANF, α-MyHC or α-cardiac troponin I (cd-TnI) antibodies. The level of expression, determined by densitometric analysis, with 1.00 given as the basal level of expression in WT CMCs, is also shown. $^{***}P < 0.0001$ *versus* untreated WT; $^{\circ\circ}P < 0.001$ and $^{\circ}P < 0.01$ *versus* untreated PKC$\theta^{-/-}$. (**C**) Trypan blue incorporation in WT and PKC$\theta^{-/-}$ CMCs, treated with or without PE in for 48 h. Parallel cultures were treated with 50 μM Leu for 30 min before being exposed to PE for 48 h, as indicated. Trypan blue-positive cells were counted (20 microscopic fields per each condition, from three independent experiments) and expressed as a percentage of the total number of cells; $^{**}P < 0.001$ and $^{***}P < 0.0001$). (**D**) TUNEL analysis in cultured WT and PKC$\theta^{-/-}$ CMCs, treated with or without PE for 48 h, as indicated. TUNEL-positive nuclei were counted (20 microscopic fields per each condition, from three independent experiments) and expressed as the percentage of the total number of nuclei ($^{*}P < 0.01$). (**E**) Western blot analysis of WT and PKC$\theta^{-/-}$ CMCs, treated with or without PE for 4 h, as indicated. The blot was incubated with the α-caspase-9 antibody (upper panel), or with the α-caspase-8 antibody (lower panel). Apoptosis-induced Jurkat cell lysate was used as the positive control (C +)

undergo stress response, as shown by the progressive increase in cell size, as well as by the upregulation of the expression of fetal genes, such as *ANF*, α-*SKA* and β-*myosin*. Indeed, the return to a pattern of fetal metabolism is considered a common feature of a hemodynamically or metabolically stressed heart.[26]

Taken together, these data suggest that ablation of PKCθ results in cardiomyocyte loss, which, in turn, promotes cardiac remodeling, fibrosis and ventricular dilation; this indicates that PKCθ is required for cardiomyocyte survival, as it has previously been shown for other cell types.[11,12] Indeed, whereas no alterations were observed in prosurvival (ERKs)

activities, an increase in proapoptotic (p38 and JNK) activities was observed in LVs lacking PKCθ. Interestingly, PKCε and PKCδ are known to activate MAP kinase signaling pathways in cardiomyocytes,[27] and the diastolic dysfunction and interstitial fibrosis observed in PKC$\varepsilon^{-/-}$ mice after pressure overload, are associated with a decrease in ERK and an increase in p38 and JNK phosphorylations, as the latter is probably dependent on PKCδ upregulation.[25] As no alteration in PKCε or PKCδ expression was observed PKC$\theta^{-/-}$ hearts, the results obtained in our study suggest that PKCθ activity is required to maintain the correct balance between MAPK pathways and, consequently, to ensure physiological cell survival. Several mouse models now show that cardiomyocyte death itself may directly cause dilated cardiomyopathy.[28] Although no supporting data are available yet, it is possible that PKCθ activity is required on one hand to counterbalance the PKCδ-dependent activation of p38 and JNK, whereas, on the other hand, to support the survival of PKCε-induced proliferating cardiomyocytes. Intriguingly, the phenotype observed in PKC$\varepsilon^{-/-}$ mice after pressure overload, wherein PKCδ is upregulated, presents many similarities to those observed in basal condition when PKCθ is ablated.[25]

In keeping with *in vivo* observations, cultured CMCs lacking PKCθ acquire a hypertrophic-like phenotype, as shown by both morphological and molecular analyses; in fact, increased accumulation of both ANF and MyHC is evident in PKC$\theta^{-/-}$ CMCs, although Akt expression and phosphorylation are not affected, suggesting that the phenotype observed is Akt independent. Surprisingly, the lack of PKCθ prevents pharmacologically induced hypertrophy; rather, cell size decreases, and the expression of *ANF* and *MyHC*, and Akt activation is prevented. Indeed, PKC$\theta^{-/-}$ CMCs are more susceptible to cell death than WT CMCs, both at basal condition and after pharmacological or environmental stress-induced stimuli. The fact that the death of PKC$\theta^{-/-}$ CMCs can be prevented by treatment with leupeptin, a protease inhibitor, shows that the observed cell death can be attributed to protease activities. It is noteworthy that leupeptin preferentially inhibits calpain activity, thereby highlighting a possible role of this class of proteases in the cell death observed in our study. Indeed, reduced expression of the regulatory myofibrillar protein cd-TnI was observed in PKC$\theta^{-/-}$. Troponins are susceptible to proteolytic degradation by intracellular proteases, such as calpain-I, caspases and matrix metalloproteinase-2, which occur in reversibly or irreversibly damaged cardiomyocytes.[29,30] As a consequence, degradation products of troponins are detected in the serum of patients with acute myocardial infarction, and it is considered as a reliable clinical cardiovascular biomarker.[31] Accordingly, TUNEL analysis shows that the observed cardiomyocyte death is mainly due to apoptosis, and, in particular, activation of the intrinsic cell death pathway, as caspase-9, but not caspase-8, cleavage was observed in PKC$\theta^{-/-}$ CMCs, and was further increased after PE exposure. The involvement of PKCθ in this pathway is supported by a number of observations in T cells wherein it is well documented that PKCθ promotes cell survival by both inhibiting the proapoptotic factor Bad and activating the antiapoptotic factor Bcl_{xL}.[11,12]

Further experiments are warranted to more accurately define the molecular mechanisms underlying the observed phenotype and the relative contribution of the PKCθ-regulated signaling pathways. PKCθ, as a member of the nPKCs subfamily, is known to mediate the nuclear export of class II HDACs, probably by regulating PKCμ/PKD activity.[15,19] Class II HDACs act as negative regulators of pathological cardiac remodeling through their association with the myocyte enhancer factor-2 transcription factor and other prohypertrophic transcriptional regulators.[32] However, recent data, based on a PKD1 conditional knock out, suggest that PKD1 is required to actually transduce stress stimuli involved in pathological cardiac remodeling *in vivo*.[33] As PKD1 is a common substrate for all members of the novel class of PKCs, it is conceivable that PKCθ may also have a specific role in the regulation of heart maintenance, besides exerting its activity on PKD functions.

In conclusion, the results reported in this paper show that PKCθ ensures cardiac muscle homeostasis, at least in part, by preventing cardiomyocyte cell death in response to work demand and neuro-hormonal signals, to which heart cells are continuously exposed. This study advances the understanding of cellular mechanisms responsible for preservation of myocardial integrity, and the observation that PKCθ can be considered a key protein for cardiac structure and function under physiological conditions, may thus be instrumental for future development of therapeutic strategies for the treatment of pathological cardiac remodeling and heart failure, using select PKCθ isoform modulators.

Materials and Methods

Animals. PKC$\theta^{-/-}$ mice (C57BL/6J background strain) were kindly provided by Littmann and colleagues.[34] For *in vivo* studies, 2-month-old male mice were used throughout the experiments, unless otherwise specified. The animals were housed in the Histology Department accredited animal facility. All the procedures were approved by the Italian Ministry for Health and conducted according to the US National Institutes of Health guidelines.

Antibodies. The following primary antibodies were used: the antimyosin heavy-chain MF20,[35] the anti-ANF (Bachem, Bubendorf, Switzerland); the anti-caveolin-3, the anti-PKC-α, -δ, -ε, -η, -θ and the anti-phospho^{Thr538} PKCθ (BD Bioscience, Franklin Lake, NJ, USA); the anti-Akt, the anti-phosphoAkt, the anti-phosphoGSK3β and the anti phospho-p38 (Cell Signalling Inc., Danvers, MA, USA); the anti-caspase-9 (Assay Designs, Ann Arbor, MI, USA); the anti-caspase-8 (Santa Cruz Biotec, Santa Cruz, CA, USA); the anti-α-tubulin (Sigma-Aldrich, St. Louis, MO, USA).

Transthoracic echocardiography. Echocardiographic analysis was performed using a high-resolution echocardiograph (VeVo 770, Visualsonics, Toronto, ON, Canada) equipped with a 33 MHz transducer. End-diastolic and end-systolic intraventricular septum (IVSTd, IVSTs), posterior wall thickness (PWTd, PWTs) and LV internal diameters (LVEDD, LVESD) were measured. Percentage fractional shortening (%FS) and relative ejection fraction (EF) were calculated using standard formulas:

$$\%FS = [(LVEDD - LVESD)/LVEDD] \times 100$$

$$EF = [(LV\ End - diastolic\ volume - LV\ End - systolic\ volume)/LV\ End - diastolic\ volume] \times 100$$

LV hemodynamics. Mice were anesthetized with an intraperitoneal injection of ketamine/xylazine (80/10 mg/kg body weight), and inotropic and lusitropic functions were evaluated by measuring intraventricular volume and pressure using a micromanometer catheter (Millar 1.4 F, SPR 671, Millar Instruments, Houston, TX, USA) positioned in the LV through right common carotid artery cannulation.[36] An estimate of systolic and diastolic LV performance was yielded by a series of pressure–volume loops of consecutive cardiac cycles.

Thoracic aortic constriction. Thoracic Aortic Constriction (TAC) was imposed between the *truncus anonymous* and the left carotid artery using a 7-0 nylon suture ligature, as described previously.[36] A separate group of mice underwent the same surgical procedures, but without aortic stenosis (sham operated). Fifteen minutes after TAC, simultaneous left and right carotid pressures were measured under anesthesia, to assess the degree of pressure load. Immediately after, the hearts were removed, the chambers dissected, weighed and processed for protein extraction.

Cell cultures. Neonatal mouse ventricular myocytes (CMCs) were isolated from the LVs of 1–3-day-old mice. In brief, cells were extracted by multiple rounds of 15 min at 37°C in ADS buffer (116 mM NaCl, 5.4 mM KCl, 18 mM HEPES, 0.9 mM Na_2HPO_4, 5.5 mM glucose, 0.4 mM $MgSO_4$, pH 7.35) containing Collagenase Type 2 (108 Units/ml, Worthington, Lakewood, NJ, USA) and Pancreatin (0.9 mg/ml, Sigma-Aldrich. The cells were then suspended in a 4 : 1 ratio of Dulbecco's modified Eagle's medium and M-199 culture medium, supplemented with 10% horse serum, 5% fetal calf serum, 2 mM glutamine (all from Gibco Invitrogen, Carlsbad, CA, USA) and 1% AraC (Sigma-Aldrich). A 90-min preplating step was performed. The final cell suspension was plated on collagen-coated dishes in a 37°C, 5% CO_2 incubator. After 24 h, the medium was replaced with serum-free medium and cells were cultured for 24 h before being exposed to treatment for the additional periods of time indicated. CFs were enriched with the preplating, and cultured on uncoated culture dishes in a 37°C, 5% CO_2 incubator.

Histological and immunofluorescence analyses. For histological analyses, heart cryosections were fixed in 4% paraformaldehyde (Sigma-Aldrich) and stained with hematoxylin/eosin or Gomori's trichrome (both from Sigma-Aldrich) solutions. Fibrotic areas were measured using the Image J software (NIH, Bethesda, MD, USA). For immunofluorescence analysis, cryosections were fixed in 4% paraformaldehyde, as described above, whereas cultured cells were fixed in ethanol/acetone (1 : 1 ratio) at −20°C for 20 min, and processed as described previously.[35] Samples were examined under a Zeiss Axioskop 2 Plus fluorescence microscope (Zeiss, Gottingen, Germany), as mentioned above. The mean CMC CSA in the heart tissue, as well as the mean cell area in cultured CMCs, were measured using the Scion Image 4.0.3.2 software (NIH, Bethesda, MD, USA). CMC number in the heart tissue was determined by counting caveolin-3 and myosin $^{+ve}$ cells per microscopic field.

Preparation of protein extracts and western blot analysis. For the total protein extract preparation, tissue samples or cell pellets were homogenized in RIPA buffer (10 mM Tris pH 7.5, 150 mM NaCl, 1% NP-40, 0.5% Na Desoxycholate, 0.1% SDS, 10% glycerol, 0.2 mM EDTA, 200 μg/ml leupeptine, 10 μg/ml aprotinine, 1 mM PMSF, 10 mM Na Fluorure, 1 mM Na Orthovanadate). For the preparation of subcellular protein fractions, LVs were homogenized in homogenization buffer (20 mM Tris pH 7.5, 2 mM EGTA, 2 mM EDTA, 250 mM sucrose, 5 mM DTT, 1 mM PMSF, 200 μg/ml Leupeptin, 10 μg/ml aprotinin) and incubated 30 min on ice. Samples were then spun at 100 000 × *g* for 30 min at 4°C. The supernatant was saved as cytosolic fraction, whereas the remaining pellet was suspended in homogenization buffer containing 0.1% Triton X-100, and incubated for 30 min on ice. At the end, the samples were spun at 100 000 × *g* for 30 min at 4°C, and the remaining supernatant was saved as the particulate fraction. An equal amount of each sample was loaded onto 10% SDS-polyacrylamide gels and transferred to a nitrocellulose membrane (Schleicher and Schuell, Dassel, Germany). The membranes were then incubated with the appropriate primary antibodies. Alkaline phosphatase-conjugated goat anti-mouse IgG (Roche Applied Science, Indianapolis, IN, USA) or alkaline phosphatase-conjugated goat anti-rabbit IgG (Zymed Laboratories, San Francisco, CA, USA) were used as secondary antibodies, and immunoreactive bands were detected with the CDP-STAR solution (Roche Applied Science), according to the manufacturer's instructions. Densitometric analysis was performed using the Aida 2.1 Image software (Raytest, Straubenhardt, Germany); α-tubulin optic density was used for normalization.

RNA preparation and RT-PCR analysis. Total RNA from cultured cells was isolated using the High Pure RNA Isolation Kit (Roche Applied Science), whereas total RNA from LVs was isolated using TRIZOL Reagent (Invitrogen), according to the manufacturers' instructions. cDNA was synthesized using the Superscript III system (Invitrogen), and PCR amplified using Taq Polymerase (Takara Bio Inc., Shiga, Japan). The sequences of primers used for PCR were as follows: α-*MyHC*, forward ACCGTCTGGACGAGGCAGAGCAGA, reverse CGTC GTGCATCTTCTTGGCACCAA (annealing temperature 62°C, expected band 420 bp); β-*MyHC*, forward CAGCACCGTCTGGACGAGGCAGAG, reverse ATTCAGGCCCTTGGCACCAATGTC (annealing temperature 62°C, expected band 420 bp); *ANF*, forward CAGAGTGGGCAGAGACAGCA, reverse TTGCTTTT CAAGAGGGCAGATCTAT (annealing temperature 65°C, expected band 389 bp); α-*cardiac actin*, forward TGTTACGTCGCCTTGGATTTTGA, reverse AAGAGAG AGACATCTCAGAAGC (annealing temperature 65°C, expected band 494 bp); α-*skeletal actin*, forward TATTCCTTCGTGACCACAGCTGAACGT, reverse CGC GAACGCAGTCGCGGGTGCGC (annealing temperature 65°C, expected band 560 bp); α*SMA*, forward TCAGGGAGTAATGGTTGGAATG, reverse TCGGCAG TAGTCACGAAGGAA (annealing temperature 58°C, expected band 495 bp); *COL1α1*, forward GGGCGAGTGCTGTGCTTTCTG, reverse CCTCGGTGTCCC TTCATTCCA (annealing temperature 58°C, expected band 537 bp); *COL3α1*, forward AGCCACCTTGGTCAGTCCTA, reverse TTCCTCCCACTCCAGACTTG (annealing temperature 55°C, expected band 403 bp); *TGFβ1*, forward CAAGGA GACGGAATACAGGGCT, reverse CGCACACAGCAGTTCTTCTCTGT (annealing temperature 55°C, expected band 260 bp); *PCNA*, forward TCCTTGGTACA GCTTACT, reverse TGCTAAGGTGTCTGCATT (annealing temperature 52°C, expected band 165 bp); *Cyclin D1*, forward GTGCCATCCATGCGGAA, reverse GGATGGTCTGCTTGTTCTCA (annealing temperature 52°C, expected band 362 bp); *GAPDH*, forward ATGTTCCAGTATGACTCCACTCACG, reverse GAGTT GCTGTTGAAGTCGCAGGAGACAA (annealing temperature 63°C, expected band 734 bp). The same reaction profile was used for all the primer sets: an initial denaturation at 95°C for 5 min, followed by 30 cycles of 95°C for 1 min; primer-specific annealing temperature for 1 min; 72°C for 2 min; finally, 7 min at 72°C. Amplification of the glyceraldehyde 3-phosphate dehydrogenase (GAPDH) housekeeping transcript was used for normalization. PCR products were separated on 1% agarose gel in a TAE buffer containing ethidium bromide, and digitized images were obtained using a CCD camera Detection System (Diana II, Raytest, Straubenhardt, Germany).

BrdU assay. Two-month-old mice were intraperitoneally injected with BrdU (25 mg/kg, Roche Applied Science). Mice were killed after 24 h, and 7 μm cryosections were prepared from the hearts. Cultured cells were incubated with BrdU labeling medium (BrdU Labeling and Detection kit I, Roche Applied Science) for 1 h and then fixed. BrdU incorporation was detected according to the manufacturer's instructions, and analyzed under an epifluorescence Zeiss Axioskop 2 Plus microscope, equipped with a CCD camera.

Cell death assays. Cell viability was determined on fixed cells stained with 0.08% trypan blue dye; nuclei were counterstained with Hoechst 33342 (Sigma-Aldrich). Cell apoptosis was determined by TUNEL reaction (Roche Applied Science). At the times indicated, cells were fixed and incubated for 1 h at 37°C with the TUNEL mixture. Positive nuclei were detected under an epifluorescence Zeiss Axioskop 2 Plus microscope, as described above.

Statistical analysis. All data are expressed as mean ± S.E.M. Statistical hypotheses were tested by Student's *t*-test or one-way ANOVA, followed by Bonferroni's *post hoc* test, as appropriate. A $P<0.01$ was considered statistically significant.

Conflict of interest

The authors declare no conflict of interest.

Acknowledgements. We thank Dr. DA Littman, NYU, NY, USA, for providing the mutant mice. We also thank Dr. M Immacolata Senni for her continuous technical support, and Dr. Lewis Baker for editing the English. This work was supported by the Italian Ministry for University and Research (2006064322_004 and 2006064322_001), by Sapienza University of Rome (C26F07MY89 and C26A08EY99), by Association Françoise contre les Myopathies, AFM (12668-2007 and 13951-2009) and by Agenzia Spaziale Italiana, ASI.

1. Selvetella G, Lembo G. Mechanisms of cardiac hypertrophy. *Heart Fail Clin* 2005; **1**: 263–273.
2. Dunnmon PM, Iwaki K, Henderson SA, Sen A, Chien KR. Phorbol esters induce immediate-early genes and activate cardiac gene transcription in neonatal rat myocardial cells. *J Mol Cell Cardiol* 1990; **22**: 901–910.

3. Allo SN, Carl LL, Morgan HE. Acceleration of growth of cultured cardiomyocytes and translocation of protein kinase C. *Am J Physiol* 1992; **263**: C319–C325.
4. Palaniyandi SS, Sun L, Ferreira JC, Mochly-Rosen D. Protein kinase C in heart failure: a therapeutic target? *Cardiovasc Res* 2009; **82**: 229–239.
5. Muth JN, Bodi I, Lewis W, Varadi G, Schwartz A. A Ca(2+)-dependent transgenic model of cardiac hypertrophy: a role for protein kinase Calpha. *Circulation* 2001; **103**: 140–147.
6. Braz JC, Bueno OF, De Windt LJ, Molkentin JD. PKC alpha regulates the hypertrophic growth of cardiomyocytes through extracellular signal-regulated kinase1/2 (ERK1/2). *J Cell Biol* 2002; **156**: 905–919.
7. Braz JC, Gregory K, Pathak A, Zhao W, Sahin B, Klevitsky R *et al.* PKC-alpha regulates cardiac contractility and propensity toward heart failure. *Nat Med* 2004; **10**: 248–254.
8. Bowman JC, Steinberg SF, Jiang T, Geenen DL, Fishman GI, Buttrick PM. Expression of protein kinase C beta in the heart causes hypertrophy in adult mice and sudden death in neonates. *J Clin Invest* 1997; **100**: 2189–2195.
9. Roman BB, Geenen DL, Leitges M, Buttrick PM. PKC-beta is not necessary for cardiac hypertrophy. *Am J Physiol Heart Circ Physiol* 2001; **280**: H2264–H2270.
10. Takeishi Y, Ping P, Bolli R, Kirkpatrick DL, Hoit BD, Walsh RA. Transgenic overexpression of constitutively active protein kinase C epsilon causes concentric cardiac hypertrophy. *Circ Res* 2000; **86**: 1218–1223.
11. Manicassamy S, Gupta S, Sun Z. Selective function of PKC-theta in T cells. *Cell Mol Immunol* 2006; **3**: 263–270.
12. Hayashi K, Altman A. Protein kinase C theta (PKCtheta): a key player in T cell life and death. *Pharmacol Res* 2007; **55**: 537–544.
13. Zappelli F, Willems D, Osada S, Ohno S, Wetsel WC, Molinaro M *et al.* The inhibition of differentiation caused by TGFbeta in fetal myoblasts is dependent upon selective expression of PKCtheta: a possible molecular basis for myoblast diversification during limb histogenesis. *Dev Biol* 1996; **180**: 156–164.
14. Serra C, Federici M, Buongiorno A, Senni MI, Morelli S, Segratella E *et al.* Transgenic mice with dominant negative PKC-theta in skeletal muscle: a new model of insulin resistance and obesity. *J Cell Physiol* 2003; **196**: 89–97.
15. D'Andrea M, Pisaniello A, Serra C, Senni MI, Castaldi L, Molinaro M *et al.* Protein kinase C theta co-operates with calcineurin in the activation of slow muscle genes in cultured myogenic cells. *J Cell Physiol* 2006; **207**: 379–388.
16. Gao Z, Wang Z, Zhang X, Butler AA, Zuberi A, Gawronska-Kozak B *et al.* Inactivation of PKCtheta leads to increased susceptibility to obesity and dietary insulin resistance in mice. *Am J Physiol Endocrinol Metab* 2007; **292**: E84–E91.
17. Baier G. The PKC gene module: molecular biosystematics to resolve its T cell functions. *Immunol Rev* 2003; **192**: 64–79.
18. De Windt LJ, Lim HW, Haq S, Force T, Molkentin JD. Calcineurin promotes protein kinase C and c-Jun NH2-terminal kinase activation in the heart. Cross-talk between cardiac hypertrophic signaling pathways. *J Biol Chem* 2000; **275**: 13571–13579.
19. Vega RB, Harrison BC, Meadows E, Roberts CR, Papst PJ, Olson EN *et al.* Protein kinases C and D mediate agonist-dependent cardiac hypertrophy through nuclear export of histone deacetylase 5. *Mol Cell Biol* 2004; **24**: 8374–8385.
20. Baines CP, Molkentin JD. STRESS signaling pathways that modulate cardiac myocyte apoptosis. *J Mol Cell Cardiol* 2005; **38**: 47–62.
21. Li L, Hessel M, van der Valk L, Bax M, van der Linden I, van der Laarse A. Partial and delayed release of troponin-I compared with the release of lactate dehydrogenase from necrotic cardiomyocytes. *Pflugers Arch* 2004; **448**: 146–152.
22. Mochly-Rosen D, Wu G, Hahn H, Osinska H, Liron T, Lorenz JN *et al.* Cardiotrophic effects of protein kinase C epsilon: analysis by *in vivo* modulation of PKCepsilon translocation. *Circ Res* 2000; **86**: 1173–1179.
23. Gray MO, Zhou HZ, Schafhalter-Zoppoth I, Zhu P, Mochly-Rosen D, Messing RO. Preservation of base-line hemodynamic function and loss of inducible cardioprotection in adult mice lacking protein kinase C epsilon. *J Biol Chem* 2004; **279**: 3596–3604.
24. Peterson KL, Skloven D, Ludbrook P, Uther JB, Ross Jr J. Comparison of isovolumic and ejection phase indices of myocardial performance in man. *Circulation* 1974; **49**: 1088–1101.
25. Klein G, Schaefer A, Hilfiker-Kleiner D, Oppermann D, Shukla P, Quint A *et al.* Increased collagen deposition and diastolic dysfunction but preserved myocardial hypertrophy after pressure overload in mice lacking PKCepsilon. *Circ Res* 2005; **96**: 748–755.
26. Rajabi M, Kassiotis C, Razeghi P, Taegtmeyer H. Return to the fetal gene program protects the stressed heart: a strong hypothesis. *Heart Fail Rev* 2007; **12**: 331–343.
27. Heidkamp MC, Bayer AL, Martin JL, Samarel AM. Differential activation of mitogen-activated protein kinase cascades and apoptosis by protein kinase C epsilon and delta in neonatal rat ventricular myocytes. *Circ Res* 2001; **89**: 882–890.
28. Movassagh M, Foo RS. Simplified apoptotic cascades. *Heart Fail Rev* 2008; **13**: 111–119.
29. Wang W, Schulze CJ, Suarez-Pinzon WL, Dyck JR, Sawicki G, Schulz R. Intracellular action of matrix metalloproteinase-2 accounts for acute myocardial ischemia and reperfusion injury. *Circulation* 2002; **106**: 1543–1549.
30. Feng J, Schaus BJ, Fallavollita JA, Lee TC, Canty Jr JM. Preload induces troponin I degradation independently of myocardial ischemia. *Circulation* 2001; **103**: 2035–2037.
31. Michielsen EC, Diris JH, Kleijnen VW, Wodzig WK, Van Dieijen-Visser MP. Investigation of release and degradation of cardiac troponin T in patients with acute myocardial infarction. *Clin Biochem* 2007; **40**: 851–855.
32. Zhang CL, McKinsey TA, Chang S, Antos CL, Hill JA, Olson EN. Class II histone deacetylases act as signal-responsive repressors of cardiac hypertrophy. *Cell* 2002; **110**: 479–488.
33. Fielitz J, Kim MS, Shelton JM, Qi X, Hill JA, Richardson JA *et al.* Requirement of protein kinase D1 for pathological cardiac remodeling. *Proc Natl Acad Sci USA* 2008; **105**: 3059–3063.
34. Sun Z, Arendt CW, Ellmeier W, Schaeffer EM, Sunshine MJ, Gandhi L *et al.* PKC-theta is required for TCR-induced NF-kappaB activation in mature but not immature T lymphocytes. *Nature* 2000; **404**: 402–407.
35. Castaldi L, Serra C, Moretti F, Messina G, Paoletti R, Sampaolesi M *et al.* Bisperoxovanadium, a phospho-tyrosine phosphatase inhibitor, reprograms myogenic cells to acquire a pluripotent, circulating phenotype. *FASEB J* 2007; **21**: 3573–3583.
36. Brancaccio M, Fratta L, Notte A, Hirsch E, Poulet R, Guazzone S *et al.* Melusin, a muscle-specific integrin beta1-interacting protein, is required to prevent cardiac failure in response to chronic pressure overload. *Nat Med* 2003; **9**: 68–75.